Biotechnol Lett (2020) 42:727–736
https://doi.org/10.1007/s10529-020-02823-2

ORIGINAL RESEARCH PAPER

Nanobody against PDL1

Shufeng Li · Kunpeng Jiang · Ting Wang · Wei Zhang · Minke Shi · Baojun Chen · Zichun Hua

Received: 9 September 2019 / Accepted: 26 January 2020 / Published online: 31 January 2020

Abstract Programmed death ligand 1 (PDL1, CD274, B7-H1) has been identified as the ligand for the immune inhibitory receptor programmed death 1 protein (PD1/PDCD1). PDL1 is a member of B7 family of immune molecules and this protein together with PDL2, are two ligands for PD1 expressed on activated lymphoid cells. By binding to PD1 on activated T cells, PDL1 may inhibit T cell responses by inducing apoptosis. Accordingly, it leads to the immune evasion of cancers and contribute to tumor growth, thus PDL1 is regarded as therapeutic target for malignant cancers. We selected PDL1 specific nanobodies from a high quality dromedary camel immune library by phage display technology, three anti-PDL1-VHHs were developed.

Keywords Nanobody · Programmed death 1 · Programmed death ligand 1 · Tumor

S. Li (✉) · K. Jiang · T. Wang · W. Zhang
Key Laboratory of Developmental Genes and Human Disease in Ministry of Education, Department of Biochemistry and Molecular Biology, Medical School of Southeast University, Nanjing 210009, China
e-mail: shufengli@seu.edu.cn

M. Shi · B. Chen
Department of Thoracic and Cardiovascular Surgery, The Affiliated Drum Tower Hospital of Nanjing University Medical School, Nanjing, China

Z. Hua
The State Key Laboratory of Pharmaceutical Biotechnology, School of Life Sciences, Nanjing University, Nanjing 210046, Jiangsu, China

Z. Hua
Changzhou High-Tech Research Institute of Nanjing University and Jiangsu Target Pharma Laboratories,Inc., Changzhou 213164, Jiangsu, People's Republic of China

Introduction

Immune checkpoints are inhibitory pathways of the immune system that maintain self-tolerance and prevent autoimmunity (Planes-Laine et al. 2019; Rosskopf et al. 2019; Tundo et al. 2019). Several inhibitory immune checkpoints have been described. The PD-1/PDL1 immune checkpoint is one of the best characterized receptor and ligand. PD1 (programmed death-1, also known as CD279), a type 1 transmembrane receptor, is expressed on the surface of activated T cells in peripheral tissues. Its ligands, programmed death-ligand 1 (PDL1, B7-H1, CD274), are commonly expressed on the surface of dendritic cells or macrophages (Zuazo et al. 2017). The binding of PD1 to its PDL1 ligand limits T cell activity, thereby preventing excessive stimulation and maintaining immune tolerance to self-antigens. However, PDL1 surface expression are often upregulated by tumor cells to induce local immune suppression and attenuate the endogenous antitumor immune response (Amarnath et al. 2011; Kythreotou et al. 2018; Munn

2018). Based on the significant regulatory effect of PDL1 on immune responses, antibodies against human PDL1 have been developed for enhancing immunological responses against cancer. The therapeutic application of PDL1/PD1 blocking antibodies has revolutionized cancer treatments (Bylicki et al. 2018; Kambayashi et al. 2019; Kwok et al. 2016).

Nanobodies are derived from heavy-chain only antibodies that occur naturally in the serum of camelids (Khodabakhsh et al. 2018). Nanobodies are also called single-domain variable heavy chain (VHH) antibody fragments. They are the smallest, intact antigen binding antibody fragments. They show excellent stability, and can easily be engineered and produced in prokaryotic cells (Rothbauer 2018). Due to their small size and unique structure, nanobodies perform better in many capture and detection applications than other antibodies. Advantageous features of nanobodies also include their high solubility, high stability, and excellent tissue penetration in vivo. With multiple competitive advantages over other formats of antibodies, nanobodies are in the interest of many researchers as well as biopharmaceutical companies for diagnostic and therapeutic applications, and they could be good replacement for traditional antibodies in future (Khodabakhsh et al. 2018; Salvador et al. 2019).

In the present work, we successfully constructed a T7 phage display cDNA library against PDL1. From the immunized camel VHH library, PDL1-specific VHH was obtained. Additionally, the selected PDL1 specific VHHs were further analyzed for their binding activity and affinity.

Current phage display systems are based on various bacteriophage vectors. The most frequently used phage display vectors are M13 and T7 phages. For M13 as a phage display platform, exogenous peptides are expressed in the M13 coat proteins, M13 phage display is depend on a protein secretion pathway and associated with limitations in the secretion of phage into the periplasm. By contrast, T7 phage expressed exogenous peptides as capsid fusion proteins, phage assembly takes place in the *E. coli* cytoplasm and mature phage are released by cell lysis. Unlike M13 systems, peptides or proteins displayed on the surface of T7 do not need to be capable of secretion through the cell membrane, which avoids problems associated with steric hindrance. Compared with M13, T7 has additional properties that make it an attractive display vector. T7 grows quickly and forms plaques within 3 h, which saves time during cloning and screening. In addition, T7 phage particle is extremely robust, and is stable to harsh conditions that inactivate other phage. This stability expands the variety of agents that can be used in biopanning selection procedures, which require that the phage remain infective. (Deng et al. 2018).

Material and methods

Cell lines

293T (human embryonic kidney cells transformed with the large T antigen, ATCC® CRL-3216^{TM}) were from ATCC.

Dromedary camel immunization

A healthy dromedary camel was immunized once a week with 0.5 mg human PDL1 protein (purchased from Sino Biological company) mixed with a same volume of Freund's complete adjuvant for the first time and Freund's incomplete adjuvant for the next 6 times. After 7 times immunization injections, 100 ml of blood of the immunized dromedary were collected. Peripheral blood lymphocytes were isolated from blood by density gradient centrifugation on Percoll. Briefly, the tubes were filled with a solution of Percoll with density of 1.1 g/ml, and 0.9% NaCl diluted blood was layered on top of the Percoll, and centrifuged for 20 min at 400×*g*, banded cells were separated, and finally the enriched lymphocytes were washed to remove percoll. Total RNA was extracted from the lymphocytes and cDNA was synthesized for the nanobody library construction use.

The camel was maintained in pasture and was thoroughly inspected and handled in accordance with established international guidelines. Experimental protocols were approved by the Institutional Animal Care and Use Committee (IACUC) of Southeast University.

Construction of the immune nanobody library

The nanobody library was constructed according to our previous studies (Li et al. 2019; Liu et al. 2017). Briefly, two-step nested PCR approach was used to amplify the variable regions of heavy-chain

immunoglobulins fragments (VHH coding gene, nanobody gene) in order to avoid contamination of VH genes. The primers sequence (nest-PCR1 up and nest-PCR1 down for the first step PCR; nest-PCR2 up and nest-PCR2 down for the second PCR) was described previously (Li et al. 2019). The first step PCR was performed using the above synthesized cDNA as template. The first PCR products contain ~ 700 bp fragments and were used as the template for the second step PCR. Then, the nanobody gene repertoire were amplified by second PCR using degenerated primers including EcoRI and HindIII restriction sites (nest-PCR2 up and nest-PCR2 down). The amplified products around 500 bp were purified and ligated into T7 Select 10-3 vector (EcoRI/HindIII linearized T7 Select10-3b vector arms were from Merck Millipore) after digesting by restriction enzymes EcoRI and HindIII. Ligation products were incubated with an in vitro packaging extract to package into phage according to the manufacturer's instructions. To determine the library size, gradient dilutions of the packaging reactions were mixed with *E. coli* BLT5403 and plated on LB plates, by counting the plaques number, the size of the library was measured. Many individual plaque were chosen randomly and used in a colony PCR to estimate the percentage of colonies with a proper insert size within our library.

Selection of nanobodies from phage display library

Nanobodies against PDL1 were selected from phage library. VHH library was amplified, 20 μg PDL1 protein was immobilized onto agarose beads, and the beads were incubated with phage library and then washed unbound phage particles with PBST (Phosphate Buffered Saline with Tween 20). A fresh exponentially growing culture of *E. coli* BLT5403 was infected with the bound phages on washed beads and incubated at 37 °C until cell lysis occurred, the bound phage particles were recovered by centrifugation. The process represented one round of biopanning and these rescued phage particles were used for the next round of panning. With three consecutive rounds of biopanning, the PDL1 specific phages were enriched gradually.

Phage ELISA

Plaque assay was performed to analyze the obtained phages after three rounds of panning. Using a sterile pipet tip to scrape up the individual plaque of interest and disperse it in a tube containing logarithmically growing host cells (OD600 = 0.6), incubate with shaking at 37 until lysis is observed. Clarify the lysate by spinning and the phage titer of recombinant phage particles in the supernatant were calculate, then selected recombinant phages were tested in single phage ELISA. Briefly, ELISA plate wells were coated with human PDL1 protein at 4 °C overnight (1 μg in 200 μl PBS), the coating solution was discarded and washed with the washing buffer (PBST, Phosphate buffered saline with Tween 20). All wells were blocked with blocking buffer (1% bovine serum albumin in PBS, 200 μl/well) for 2 h and the plate was washed. 10^8 pfu of selected phages were added per well for 2 h and washed, then followed by incubation with diluted rabbit anti-T7 antibody for another 1 h and subsequently incubated with HRP-conjugated antibody. The bound recombinant phage particles were detected by adding TMB substrate solution. Finally absorbance value at 450 nm was read by using an ELISA reader. Values were the means of three replicates. Finally, fifteen positive plaques (with binding ratios relative to a non-coated well of more than 2) determined by single-phage ELISA was cultured, the phage DNA was extracted and PCR was performed to amplify the region surrounding the multiple cloning site. Sequencing of PCR product can provide the inserted VHH sequence of selected phage recombinants.

Expression and purification of anti-PDL1 nanobody

PCR amplified anti-PDL1 nanobody genes were cloned into pET32a (+) plasmid and the cloned anti-PDL1 VHH genes in recombinant plasmid of pET32a (+)-VHH was checked by sequencing. For anti-PDL1 nanobody expression, the recombinant plasmid of pET32a (+)-VHH was transformed into *E. coli* BL21 (DE3). The transformed *E. coli* BL21 was selected and cultured at 37 °C in medium until the OD_{600} reached 0.6. By adding 1 mM IPTG, expression of anti- PDL1 nanobodies were induced. Then the culture was centrifuged, the cell pellet was resuspended in lysis

buffer and sonicated. Nanobodies were purified by immobilized metal affinity chromatography (IMAC) by NI-NTA columns (HisPur™ Ni-NTA Resin, ThermoFisher Scientific) in a gradient of increasing imidazole concentration(lysis buffer:10 mM imidazole, pH 8.0; wash buffer: 50 mM imidazole, pH 8.0; elution buffer 250 mM imidazole, pH 8.0). The purity of eluted proteins was checked by sodium dodecyl sulfate-polyacrylamide gel electrophoresis (SDS-PAGE) using coomassie blue staining. Then the collected nanobodies were dialyzed in PBS buffer and applied to a gel filtration column (Superdex 75 HR 10/30 column equilibrated in 20 mM Tris–HCl pH 7.5, 150 mM NaCl, GE Healthcare). The collected fractions containing 99% pure nanobody were pooled and concentrated using an ultrafiltration unit (3000 molecular weight cutoff, Millipore).

The affinity constant (Kaff) of nanobody for binding to PDL1

The affinity constant of nanobody was determined as previously described (Beatty et al. 1987; Zhang et al. 2013). The plates were coated with PDL1 of three concentrations 5 μg/ml, 2.5 μg/ml and 1.25 μg/ml, then added and incubated with serial diluted concentrations of nanobodies. After washing, anti-HA tag mouse antibody was added, then followed by another washing, horseradish peroxidase (HRP)-conjugated goat anti-mouse IgG was added and incubated, the color was developed by the addition of substrate TMB solution. The absorbance values at 450 nm was measured. Three curves were plotted for the absorbance values versus antibody dilution. The antibody concentration resulting in 50% of the maximum absorbance value at a particular antigen coating concentration was designated as [Ab]t and selected for the affinity calculation, three [Ab]t values were obtained against three different concentrations of PDL1, and three K values were calculated according to the Beatty formula, the final affinity constant is the average result of three K values.

Cross-reactivity assay

The specificity of nanobody was characterized via ELISA, 100 μl different PDL1 (human PDL1, monkey PDL1 and mouse PDL1 were all purchased from Sino Biological company) or PDL2 proteins (human PDL2, Sino Biological company) (each 2 μg/ml in PBS) were coated on high binding plates (Corning), and a control was set. After washing and blocking, 100 μl purified anti-PDL1 VHHs at the concentration of 2 μg/ml (diluted in PBS) were incubated to detect the specificity and then followed by incubation with anti-HA tag mouse monoclonal antibody and HRP conjugated goat anti-mouse IgG. Color was developed with TMB and the signal was read at 450 nm. All analysis were repeated three times.

Western

Standard procedures of western blotting were used to determine the reactivity of the nanobody to the whole cell lysates of 293T cells transfected with pCMV-PDL1-flag on a 12% gel. The cell lysates of 293T cells transfected with empty vector pCMV-flag was used as negative control. Immunodetection was performed using VHHs or anti-flag commercial antibodies (BD Biosciences) as the primary antibody. The final signals were developed with Pierce ECL Western Blotting Substrate according to standard procedures.

Immunofluorescence staining

293T cells were seeded in plates and transfected with pCMV-PDL1-flag plasmid DNA. Transfected 293T cells were seeded on coverslips, and fixed with 4% formaldehyde in PBS for 15 min, permeabilized with 0.1% Triton X-100 for 10 min, and blocked with 5% BSA for 1 h. Successively, cells were incubated for 1 h at 37 °C in HA-tagged anti-PDL1 nanobodies and followed by the mouse anti-HA antibody incubation. The commercial anti-flag antibody was used for positive control, or left without primary antibody for negative control. Then all groups were incubated with FITC-conjugated anti mouse antibody. Finally, cells were stained with DAPI for nuclear visualization, and assessed by Olympus fluorescence microscopy.

Results

Construction of phage display nanobody library

The scheme of nanobody library construction was shown in Fig. 1a. The heavy-chain antibody variable

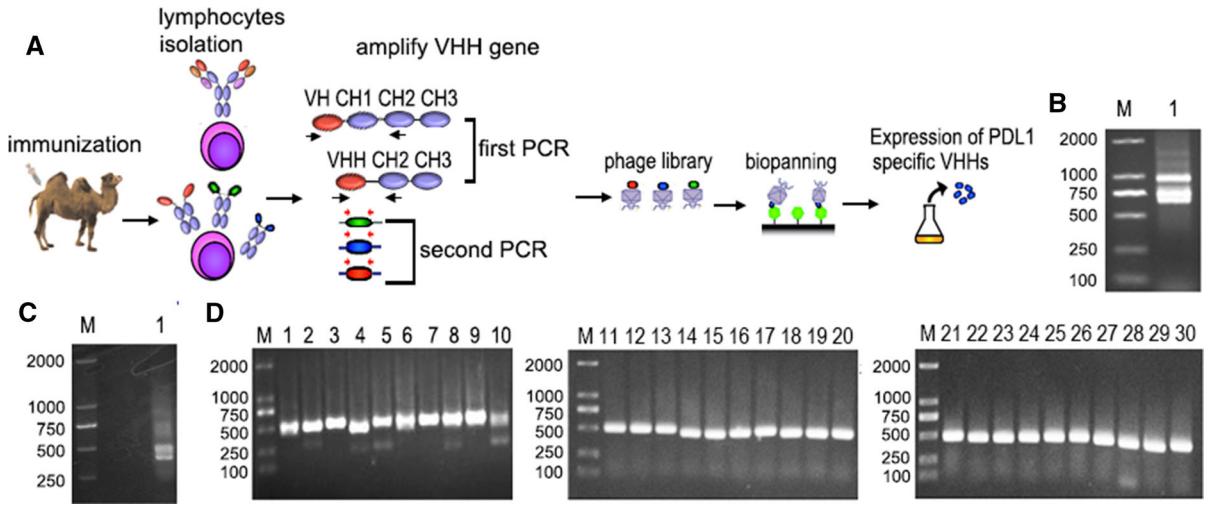

Fig. 1 Library construction. **a** Schematic showing immunization and isolation of candidate PDL1 specific VHHs. **b** The first round PCR fragments had evident bands around 900 bp and 700 bp. **c** VHH genes about 500 bp were amplified by second PCR. **d** Plaques were randomly selected to detect the percentage of phage containing an insert of VHH

region (also known as VHH) sequences were amplified from lymphocyte cDNA of the camel. The first round PCR products were analyzed by agarose gel electrophoresis, which included a 900 bp fragment for VH-CH1-CH2 exons and 700 bp for VHH-CH2 exons (Fig. 1b). Gel plugs from the bands near 700 base pairs (bp) were cut to extract DNA, the extracted DNA was used as template in the secondary PCR. This was performed with the primers nest-PCR2 up and nest-PCR2 down. The gene for the VHH domain of about 500 bp (Fig. 1c) was amplified. The VHH library against PDL1 was generated by inserting the final PCR fragments into the T7 vector and followed by in vitro packaging. Plaque assay was performed to calculate the titer of packaged phage. Size of the library was determined by counting the number of plaques after serial dilutions and plating on plates. The capacity of the library in the packaging reaction was 5×10^7pfu. Meanwhile, 30 lysis plaques were chosen for screening by PCR (Fig. 1d). The result suggested that 100% of the plaques contained the insert of the expected size for camel VHH gene. Packaged library was amplified by infection of host BLT5403.

Biopanning of phage display library against PDL1

After three rounds of panning (Table 1), PDL1 specific VHHs were enriched. To isolate VHH antibodies with high affinity and their coding sequences, 50 individual plaques from the panned library were chosen randomly and analyzed by phage ELISA. Totally 15 plaques gave a high absorbance value (with binding ratios relative to a non-coated well of more than 2) in phage ELISA (Fig. 2a). These 15 plaques were performed colony PCR to obtain the inserted sequence of PDL1 specific VHH. After PCR and sequencing, their deduced amino acid sequences were illustrated in Fig. 2b, and these phage-displayed PDL1-specific antibodies were classified according to the diversity of amino acid sequences and named VHH1, VHH2, and VHH3. Of 15 plaques sequenced, the sequence of VHH2 repeated 7 times, VHH1 repeated 3 times; and VHH3 repeat 5 times. The isolated VHH1 and VHH3 sequences had relatively longer predicted CDR3 regions (20 and 21 amino acids).

Expression and purification of PDL1 specific VHHs

Three VHH DNA sequences from the isolated plaques were inserted into the vector, and transformed into BL21 (DE3) cells. After inducion with IPTG, the 35 kDa protein band was clearly present in the induced *E. coli* containing the recombinant plasmid of pET32a (+)-VHHs, as indicated on SDS-PAGE stained with coomassie blue (Fig. 3a). Then the culture was centrifuged, the cell pellet was harvested and

Table 1 Enrichment of phages with biopanning

Rounds of panning	Input of phages (pfu)	Output of phages (pfu)	Ratio (%)
1	2×10^9	5.4×10^4	2.7×10^{-5}
2	2×10^9	1.8×10^6	9.0×10^{-4}
3	2×10^9	8.5×10^6	4.3×10^{-3}

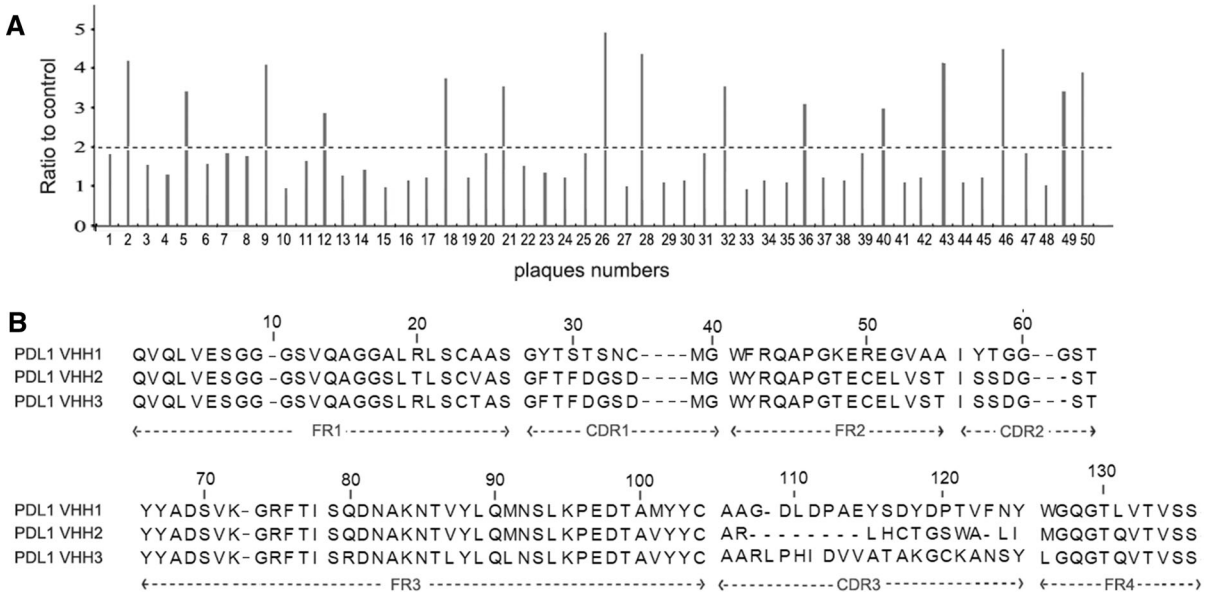

Fig. 2 Selection of nanobodies against PDL1 by phage display library. **a** Phage ELISA of randomly selected individual plaques toward PDL1. Fifty phage plaques were selected from the panned library and detected by phage ELISA. Fifteen plaques gave a high absorbance value toward PDL1 were selected. **b** Three kinds of anti-PDL1 VHHs with different amino acid sequences were identified. Numbering and CDR designations were grouped according to the methods of the international ImMunoGeneTics information system (IMGT) numbering system

sonicated. The expressed nanobodies were purified by NI-NTA columns and visualized by SDS-PAGE. The yield of anti-PDL1 VHHs were ranged from 9.2 to 20.5 mg/l culture (Fig. 3b).

Determination of affinity constants and binding specificity

The affinity constants of three nanobodies for binding to PDL1 were determined by ELISA. According to Beatty, three different concentrations of PDL1 (coated to the plate) and serial dilutions of antibody were used for ELISA, thereby enabling the calculation of three different Kaff values, which generate the average affinity constant. The affinity graphs of nanobodies were shown in Fig. 4. The kaff of VHH1, VHH2 and VHH3 was 7.5×10^7M-, 1.2×10^8M- and 1.7×10^8M- respectively.

We further tested the specificity of nanobody against PDL1 by the ELISA experiments and BSA was used as negative controls (Fig. 5a), the binding activity was estimated with several antigens, such as human PDL1 protein, monkey PDL1 protein, mouse PDL1 protein and human PDL2 protein. Except for monkey PDL1, which shows a binding activity with VHHs, no other cross activity was detected in the ELISA experiments.

Western blotting was applied to analyze the flag-PDL1 expressed in 293T cells using nanobody VHH1, VHH2 and VHH3. Obviously, three nanobodies were only reactive against their specific PDL1 antigens in 293T cells. The reactivity and specificity of anti-PDL1 nanobodies in western blotting were comparable with commercial anti-flag monoclonal antibodies, they all can recognize their specific antigens (Fig. 5b). Finally, we performed an immunofluorescence experiment to

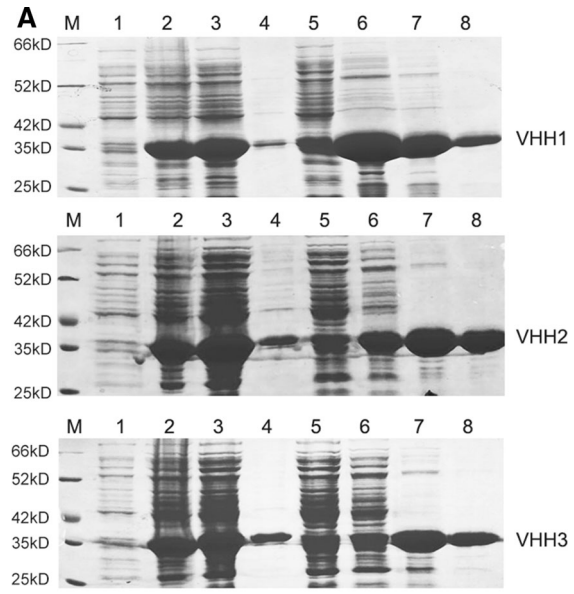

B

VHH	Yield(mg/liter)
VHH1	20.5
VHH2	17.8
VHH3	9.2

Fig. 3 Expression and purification of PDL1 specific nanobodies. **a** Three nanobodies with different sequences were expressed in *E.coli* and purified by immobilized metal affinity chromatography (IMAC). Lane M, molecular weight markers; lane 1, Total protein before IPTG induction of pet32a-VHH transformed BL21 (DE3) cells.; lane 2, Total protein of IPTG induced culture of pet32a-VHH transformed BL21(DE3) cells, showing the anti-PDL1 VHH band at 35 kDa. lane 3, Supernatant after ultrasonication; lane 4, Precipitation after ultrasonication; lane 5, The flow-through fraction; lane 6,7, The wash fraction at 50 mM imidazole; lane 8, The elution fraction at 250 mM imidazole. **b** Yield of three nanobodies

investigate the ability of anti-PDL1 VHH antibodies to access and bind PDL1 on the cell membrane. Cultured 293T cells were transfected with plasmid for the expression of PDL1, cells on cover slips were subjected to immunofluorescence staining and analzed by fluorescence microscopy. The representative image showed green fluorescence at membrane, indicating efficient recognition by anti-PDL1 VHH antibodies or commercial anti-flag antibody in combination with FITC secondary antibody (Fig. 5c). No significant background was detected in nontransfected cells or in negative control group (without primary antibody). The efficient binding of membrane PDL1 by the anti-PDL1 VHHs demonstrated that their affinity and specificity were sufficient for their application in cell PDL1 recognition.

Discussion

PDL1 was expressed on a number of cancer cells to downregulate antitumor immune responses of T cells. To block PDL1 activity and rescue T cells from inhibition, blocking antibodies has attracted attention in immunotherapy. Disruption of immune checkpoint interactions by monoclonal antibodies (mAb) has replaced chemotherapy as the standard of care for metastatic melanoma and is similarly promising in the treatment of other cancers (Larkin et al. 2015).For example, checkpoint blockade Pembrolizumab (Keytruda) has been extensively investigated in numerous malignancies.

As an alternative to full-sized antibodies, we developed camelid-derived heavy chain-only antibody fragments (VHHs) against PDL1. Nanobodies are a novel and unique class of antigen-binding fragments. Their superior properties such as small size, high stability, strong antigen-binding affinity, water solubility and natural origin led to the development of a new generation of biodrugs. Although not of human origin and frequently 'humanised', nanobodies are rarely immunogenic due to their small size and similarities with the human VH3 gene family (Harmsen and Haard 2007). A number of nanobodies have been identified and reached advanced preclinical stages, while several of them are currently being tested in clinical trials (Jovčevska and Mulydermanas 2019). Recently, caplacizumab, a bivalent nanobody, received approval from the European Medicines Agency (EMA) and the US Food and Drug Administration (FDA) for treatment of patients with thrombotic thrombocytopenic purpura by targeting von Willebrand factor (vWF) (Poullin et al. 2019)

Another promising application of nanobodies is the use as targeting ligands for nanobodies-mediated tumor drug delivery. PDL1 was mainly overexpresses in various tumor cells, rendering anti-PDL1 as a potential targeting ligand for drug delivery. Nanobodies can be easily conjugated to a variety of agents (van Brussel et al. 2016; van Lith et al. 2017). The small size and low immunogenicity of PDL1 nanobodies could offer unique benefit for serving as a targeting ligand. Recently, it was reported that fusions of the

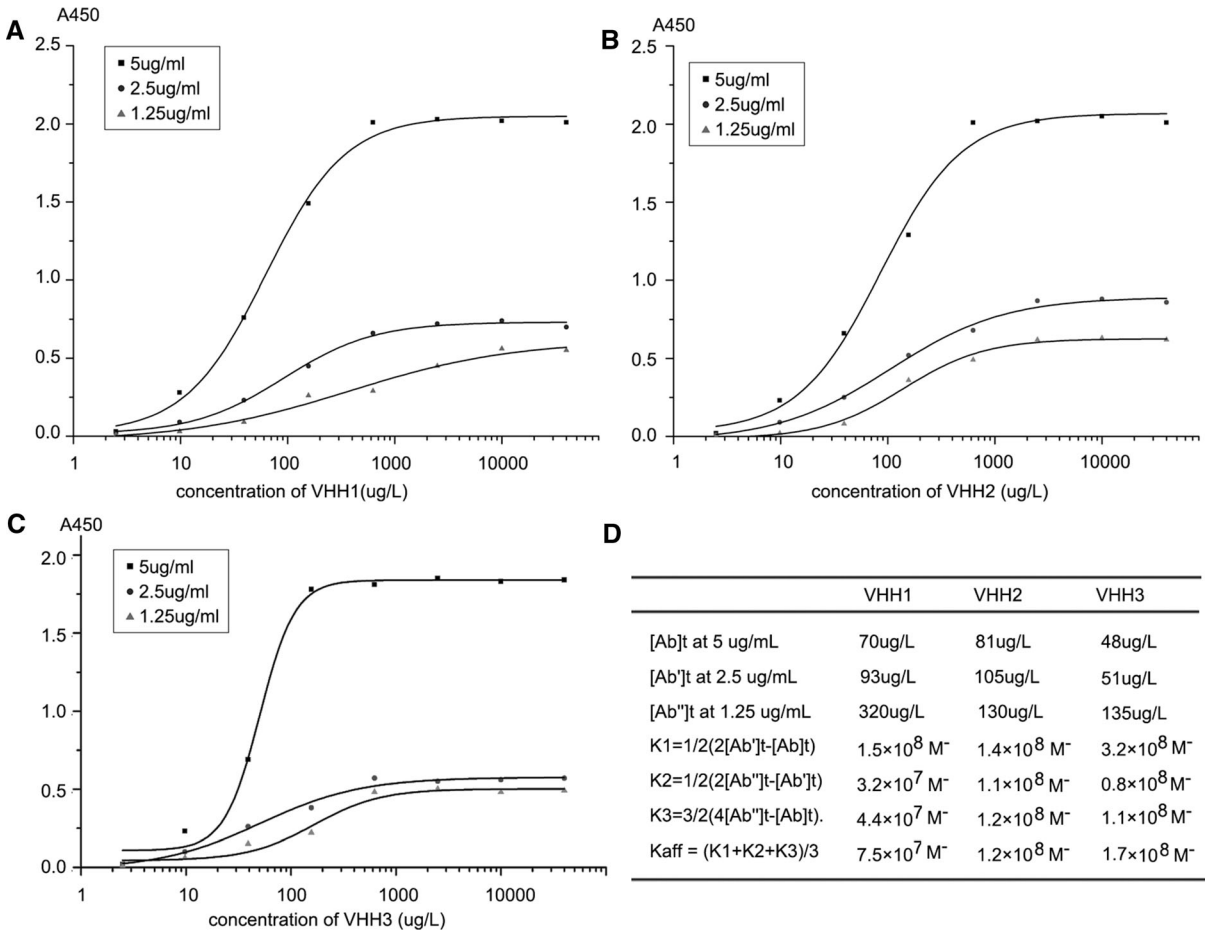

	VHH1	VHH2	VHH3
[Ab]t at 5 ug/mL	70ug/L	81ug/L	48ug/L
[Ab']t at 2.5 ug/mL	93ug/L	105ug/L	51ug/L
[Ab'']t at 1.25 ug/mL	320ug/L	130ug/L	135ug/L
K1=1/2(2[Ab']t-[Ab]t)	1.5×10^{8} M^{-}	1.4×10^{8} M^{-}	3.2×10^{8} M^{-}
K2=1/2(2[Ab'']t-[Ab']t)	3.2×10^{7} M^{-}	1.1×10^{8} M^{-}	0.8×10^{8} M^{-}
K3=3/2(4[Ab'']t-[Ab]t).	4.4×10^{7} M^{-}	1.2×10^{8} M^{-}	1.1×10^{8} M^{-}
Kaff = (K1+K2+K3)/3	7.5×10^{7} M^{-}	1.2×10^{8} M^{-}	1.7×10^{8} M^{-}

Fig. 4 The affinity constant of nanobodies for binding to PDL1 were determined by ELISA. The antibody concentration resulting in 50% of the maximum absorbance value at a particular antigen coating concentration was measured and designated as [Ab]t. Three [Ab]t values were obtained against three different concentrations of PDL1 ([Ab]t at 5 μg/ml, [Ab']t at 2.5 μg/ml and [Ab'']t at 1.25 μg/ml) and were used for the calculation of three K values according to the Beatty formula. The final affinity constant is the average result of three calculations. **a–c** experimental dose-response curves for anti-PDL1 VHHs at three different PDL1 coating concentrations. **d** Calculation of the affinity constants for anti-PDL1 VHHs

anti–PDL1 VHH with IL-2 or IFNγ was generated to direct these fusions to the tumor and reduced pancreatic tumor size (Dougan et al. 2018). Thus anti-PDL1 VHH based therapies are promising.

In current study, we immunized a dromedary camel with the human PDL1 protein, leading to the isolation of three single domain antibodies (VHHs), termed VHH1,VHH2 and VHH3. The four conservative hallmark residues in FR2 were Phe42 (or Tyr), Glu49, Arg50 (or Cys) and Gly52 (or Leu), which was consistent to previously reported distinct feature of VHHs (Li 2014; Arbabi et al. 1997). In addition, all three anti-PDL1-VHHs contain the strictly conserved intradomain disulphide bridge (cysteine 23 in FR1 and cysteine 104 in FR3), which is characteristic for the immunoglobulin fold. For VHH2 and VHH3, a second disulfide bridge is probably formed between the CDR3 and a cysteine at position 50. VHH1 here did not contain a cysteine in the CDR3. The presence of a second disulphide bond is common occurrence in VHHs of the dromedary (Dumoulin et al. 2002). Furthermore, the CDR3 with lengths of 20, 12 and 21 amino acids, do not share any sequence similarity. The sequence information of these three VHHs showed that different VHH germline genes were used.

The affinity experiment was conducted by non-competitive ELISA according to the procedure of Beatty et al. (1987) .The calculated binding affinity for

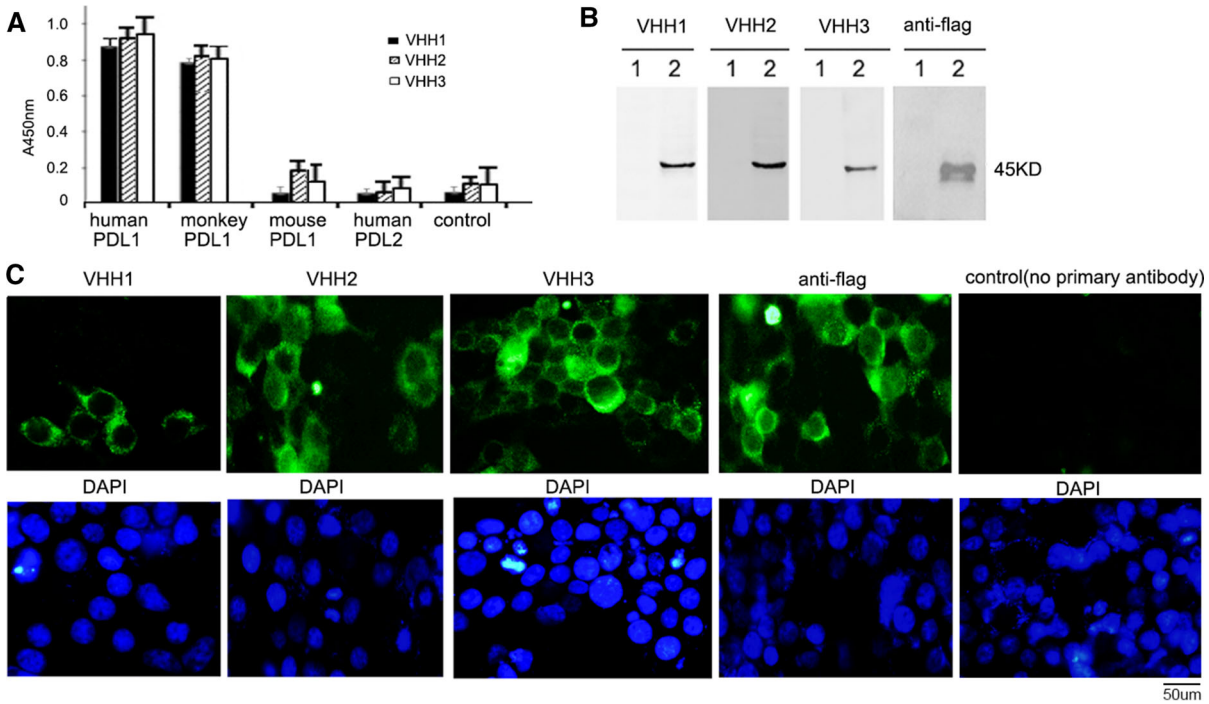

Fig. 5 Specificity of the nanobodies to human PDL1 proteins. **a** Cross-reactivity analysis based on ELISA revealed nanobodies were specific against PDL1. The PDL1 and PDL2 protein were coated, and BSA was used as control. After incubation with nanobodies, anti-HA tag mouse monoclonal antibody was added, and then anti-mouse antibody was used for detection. Finally, absorbance at 450 nm was read. **b** Western blot showed that anti-PDL1 nanobodies can recognize the PDL1 protein expressed in the pCMV- PDL1-flag transfected 293T cells. Lane1 : control cell lysates from 293T cells ; lane 2 : cell lysates from pCMV- PDL1-flag transfected 293T cells. **c** Reactivity and specificity of the three anti-PDL1 nanobodies were tested by immunofluorescence staining. 293T cells were transfected with the plasmids pCMV- PDL1-flag and submitted to immunofluorescence staining analysis using three nanobodies and commercial monoclonal antibodies (anti-flag) or left without primary antibody for the negative control. Scale bar, 50 μm

three anti-PDL1 VHHs were in the range of 7.5×10^7 M- to 1.7×10^8 M-, indicating that three nanobodies and PDL1 antigen can interact with high affinity, and VHH3 showed the highest affinity. In conclusion, their easy expression and purification, as well as high affinity and specificity to PDL1, make them useful reagents for PDL1 recognition. Further study may extend the application scope of these selected VHHs.

Acknowledgements This work was supported by grant from the Chinese National Nature Science Foundation (31070706) and by the Fund from the Applied Basic Research Programs of Science and Technology Commission Foundation of Jiangsu Province (BK20161416).

Compliance with ethical standards

Conflict of interest The authors have no conflict of interest.

References

Amarnath S, Mangus CW, Wang JC et al (2011) The PDL1-PD1 axis converts human TH1 cells into regulatory T cells. Sci Transl Med 3(111):111–120

Arbabi Ghahroudi M, Desmyter A, Wyns L, Hamers R, Muyldermans S (1997) Selection and identification of single domain antibody fragments from camel heavy-chain antibodies. FEBS Lett 414(3):521–526

Beatty JD, Beatty BG, Vlahos WG (1987) Measurement of monoclonal antibody affinity by non-competitive enzyme immunoassay. J Immunol Methods 100:173–179

Bylicki O, Paleiron N, Rousseau-Bussac G, Chouaïd C (2018) New PDL1 inhibitors for non-small cell lung cancer: focus on pembrolizumab. OncoTargets Ther 11:4051–4064

Deng X, Wang L, You X, Dai P, Zeng Y (2018) Advances in the T7 phage display system (Review). Mol Med Rep 17(1):714–720

Dougan M, Ingram JR, Jeong HJ et al (2018) Targeting cytokine therapy to the pancreatic tumor microenvironment using PDL1-specific VHHs. Cancer Immunol Res 6(4):389–401

Dumoulin M, Conrath K, Van Meirhaeghe A et al (2002) Single-domain antibody fragments with high conformational stability. Protein Sci 11(3):500–515

Harmsen MM, De Haard HJ (2007) Properties, production, and applications of camelid single-domain antibody fragments. Appl Microbiol Biotechnol 77:13–22

Jovčevska I, Muyldermans S (2019) The therapeutic potential of nanobodies. BioDrugs.https://doi.org/10.1007/s40259-019-00392-z

Kambayashi Y, Fujimura T, Hidaka T, Aiba S (2019) Biomarkers for predicting efficacies of anti-PD1 antibodies. Front Med (Lausanne) 6:174

Khodabakhsh F, Behdani M, Rami A, Kazemi-Lomedasht F (2018) Single-domain antibodies or nanobodies: a class of next-generation antibodies. Int Rev Immunol 37(6):316–322

Kwok G, Yau TC, Chiu JW, Tse E, Kwong YL (2016) Pembrolizumab (Keytruda). Hum Vaccin Immunother 12(11):2777–2789

Kythreotou A, Siddique A, Mauri FA, Bower M, Pinato DJ (2018) PDL1. J Clin Pathol 71(3):189–194

Larkin J, Chiarion-Sileni V, Gonzalez R, Grob JJ, Cowey CL, Lao CD et al (2015) Combined nivolumab and ipilimumab or monotherapy in untreated melanoma. N Engl J Med 373:23–34

Li H, Sun Y, Elseviers J et al (2014) A nanobody-based electrochemiluminescent immunosensor for sensitive detection of human procalcitonin. Analyst 139(15):3718–3721

Li S, Zhang W, Jiang K et al (2019) Nanobody against the E7 oncoprotein of human papillomavirus 16. Mol Immunol 109:12–19

Liu A, Shan H, Ma, Meng et al (2017) An ultrasensitive photoelectrochemical immunosensor by integration of nanobody, TiO2 nanorod arrays and ZnS nanoparticles for the detection of tumor necrosis factor-α. J Electroanal Chem 803:1–10

Munn DH (2018) The host protecting the tumor from the host-targeting PD–L1 expressed by host cells. J Clin Invest 128(2):570–572

Planes-Laine G, Rochigneux P, Bertucci F, Chrétien AS, Viens P, Sabatier R, Gonçalves A (2019) PD-1/PDL1 targeting in breast cancer: the first clinical evidences are emerging. A literature review. Cancers (Basel) 11:1033

Poullin P, Bornet C, Veyradier A, Coppo P (2019) Caplacizumab to treat immune-mediated thrombotic thrombocytopenic purpura. Drugs Today 55(6):367

Rosskopf S, Leitner J, Zlabinger GJ, Steinberger P (2019) CTLA-4 antibody ipilimumab negatively affects CD4 + T-cell responses in vitro. Cancer Immunol Immunother 68(8):1359–1368

Rothbauer U (2018) Speed up to find the right ones: rapid discovery of functional nanobodies. Nat Struct Mol Biol 25(3):199–201

Salvador JP, Vilaplana L, Marco MP (2019) Nanobody: outstanding features for diagnostic and therapeutic applications. Anal Bioanal Chem 411(9):1703–1713

Tundo GR, Sbardella D, Lacal PM, Graziani G, Marini S (2019) On the horizon: targeting next-generation immune checkpoints for cancer treatment. Chemotherapy 6:1–19

van Brussel AS, Adams A, Oliveira S (2016) Hypoxia-targeting fluorescent nanobodies for optical molecular imaging of pre-invasive breast cancer. Mol Imaging Biol 18(4):535–544

van Lith SAM, van den Brand D, Wallbrecher R, van Duijnhoven SMJ, Brock R, Leenders WPJ (2017) A conjugate of an anti-epidermal growth factor receptor (EGFR) VHH and a cell-penetrating peptide drives receptor internalization and blocks EGFR activation. Chembiochem 18(24):2390–2394

Zhang Y, Bao H, Miao F et al (2013) Characterization of a monoclonal antibody to Spiroplasma eriocheiris and identification of a motif expressed by the pathogen. Vet Microbiol 161(3–4):353–358

Zuazo M, Gato-Cañas M, Llorente N et al (2017) Molecular mechanisms of programmed cell death-1 dependent T cell suppression: relevance for immunotherapy. Ann Transl Med 5:385